Estimating Planetary Boundary Layer Heights from NOAA Profiler Network Wind Profiler Data

A. MOLOD*

NASA Goddard Space Flight Center, Greenbelt, Maryland

H. SALMUN+

Hunter College of the City University of New York, New York, New York

M. DEMPSEY

Earth and Environmental Sciences, Graduate Center, City University of New York, New York, New York

(Manuscript received 14 August 2014, in final form 11 May 2015)

ABSTRACT

An algorithm was developed to estimate planetary boundary layer (PBL) heights from hourly archived wind profiler data from the NOAA Profiler Network (NPN) sites located throughout the central United States. Unlike previous studies, the present algorithm has been applied to a long record of publicly available wind profiler signal backscatter data. Under clear-sky conditions, summertime averaged hourly time series of PBL heights compare well with Richardson number–based estimates at the few NPN stations with hourly temperature measurements. Comparisons with estimates based on clear-sky reanalysis show that the wind profiler (WP) PBL heights are lower by approximately 250–500 m. The geographical distribution of daily maximum PBL heights corresponds well with the expected distribution based on patterns of surface temperature and soil moisture. Wind profiler PBL heights were also estimated under mostly cloudy-sky conditions, and are generally comparable to the Richardson number–based PBL heights and higher than the reanalysis PBL heights. WP PBL heights have a smaller clear–cloudy condition difference than either of the other two. The algorithm presented here is shown to provide a reliable summertime climatology of daytime hourly PBL heights throughout the central United States.

1. Introduction

The planetary boundary layer (PBL) is the shallow layer of the troposphere nearest to the earth's surface that, particularly over land, exhibits a diurnal variation due to the exchange of energy and momentum between the surface and the atmosphere. The depth of the PBL can range from less than 100 m to several kilometers. Knowledge of the PBL depth and its fluctuations in time are essential for the estimation of the transport of atmospheric constituents, and in particular for estimating the terms in the atmospheric carbon budget (Denning et al. 1999).

Many methods exist for measuring the PBL depth, including the use of radiosondes (Seidel at al. 2010; Liu and Liang 2010), aircraft (Spangler and Dirks 1974), sodar (Beyrich 1997), wind profilers (Angevine et al. 1994), lidar (Lammert and Bösenberg 2006; Lewis et al. 2013), and global positioning system (GPS) radio occultation (Guo et al. 2011; Ao et al. 2012). Each of these methods comes with its own advantages and limitations, so the best option is to use some combination of methods (Seibert et al. 2000). For instance, radiosonde ascents, while performed operationally in numerous locations across the world, are generally limited to twice per day.

* Additional affiliation: Earth System Science Interdisciplinary Center, University of Maryland, College Park, College Park, Maryland.

+ Additional affiliation: Earth and Environmental Sciences, Graduate Center, City University of New York, New York, New York.

Corresponding author address: Andrea Molod, NASA Goddard Space Flight Center, 8800 Greenbelt Rd., Greenbelt, MD 20771.
E-mail: andrea.molod@nasa.gov

DOI: 10.1175/JTECH-D-14-00155.1

© 2015 American Meteorological Society

Aircraft sampling provides spatial information that is useful, but it is generally limited to particular regions or specific campaigns and is quite expensive. Lidar has a very high sampling rate, but it is limited in that it cannot remain unattended for long periods of time. Wind profilers are quite useful for measuring PBL depths because they can be left unattended for extended time periods, can provide a continuous stream of data over time, and there is an extensive network of operational wind profiler stations in some regions of the world. The operational wind profilers are, however, limited by the fact that there is generally no sampling below 500 m above the earth's surface.

One of the earliest successful algorithms to compute PBL height using wind profiler signal-to-noise ratio (SNR) measurements was developed by Angevine et al. (1994). Their algorithm was tested using data from a site in Alabama during June 1992. They determined the column maximum SNR every 6 min and took the median of these values for the half hour before and after a given hour and used the median as the height of the PBL. The median was used instead of the mean so as not to give outliers any great emphasis. The algorithm included a technique to remove spurious high values of SNR due to ground clutter.

Bianco and Wilczak (2002) developed a PBL height algorithm using wind profiler SNR that was designed to improve on the shortcomings of the algorithm of Angevine et al. (1994). They developed a fuzzy logic algorithm to improve on the elimination of ground clutter and another fuzzy logic algorithm to determine the depth of PBL. The second algorithm uses measures of the peak, gradient, curvature, and variance of the hourly median SNR profile along with the variance of the vertical velocity. The fuzzy logic functions were developed using data from a site in California and tested against data from a site near Houston, Texas. The fuzzy logic algorithm showed marked improvements relative to Angevine et al. (1994), particularly in the early morning hours.

Bianco et al. (2008) improved on Bianco and Wilczak's (2002) methodology for selecting PBL heights by modifying the fuzzy logic algorithm to eliminate ground clutter, and by utilizing the Doppler spectral width to clarify which of multiple maxima in the profile of SNRs correspond to the PBL height. The Doppler spectral width is sensitive to small-scale turbulent fluctuations and was used to detect the presence of an entrainment zone near the top of a growing boundary layer. The modified algorithm was applied to both clear and cloudy boundary layers at sites in Pittsburgh, Pennsylvania, and Plymouth, Massachusetts, and was shown to improve PBL estimates on clear days relative to a subjective PBL height determination, but it did not perform as well on cloudy days. Heo et al. (2003) also addressed the issue of multiple maxima utilizing the Doppler spectral width.

The covariance wavelet transform (CWT) method, previously used for estimating PBL heights from lidar data (Cohn and Angevine 2000; Lewis et al. 2013), was used by Compton et al. (2013) to estimate PBL heights from wind profiler data collected near Beltsville, Maryland, during July 2011. Their results showed that the CWT method can successfully determine PBL height as compared to radiosonde and lidar PBL height estimates, although some special treatment of early morning SNR data was needed to avoid spurious PBL heights.

In the present study, a new algorithm using archived wind profiler signal data to estimate PBL heights is presented. Data are from the NOAA Profiler Network (NPN) sites located mostly throughout the central United States. Our study uses data from approximately 30 NPN stations during the months of June–August of 2000–05. The summer study period ensures that the PBL height is in the range of the wind profiler detector for the longest time during each day. The new algorithm relies on the existence of publicly available backscatter signal data (SNR is not archived), is relatively simple and therefore not site-specific, and is potentially more robust. Following this introduction, section 2 describes the various data sources used to develop, test, and validate the algorithm to estimate PBL heights, and section 3 describes in detail the algorithm developed here. An analysis of the algorithm's performance and results under clear and mostly cloudy conditions is discussed in section 4, and the study and results are summarized in section 5.

2. Data for PBL height estimation and validation

a. *Wind profilers*

Wind profiler data were obtained from the NPN archive site (http://www.profiler.noaa.gov/npn/index.jsp). The majority of the NPN stations are in the central United States, and our study is restricted to that region. The locations of the 31 stations in the study region are marked in Fig. 1. Our study period is June–August of 2000–05. The wind profilers that are part of the NPN are ultrahigh-frequency (UHF) active remote sensing Doppler radars, operating in a frequency range of 404 MHz in general, with one instrument at 449 MHz. The NPN wind profilers operate with range gates spaced 250 m apart in the vertical, beginning at 500 m above the surface. The profilers record backscatter and signal-to-noise ratios every 6 min, but the archive consists of hourly averages of the signal backscatter only.

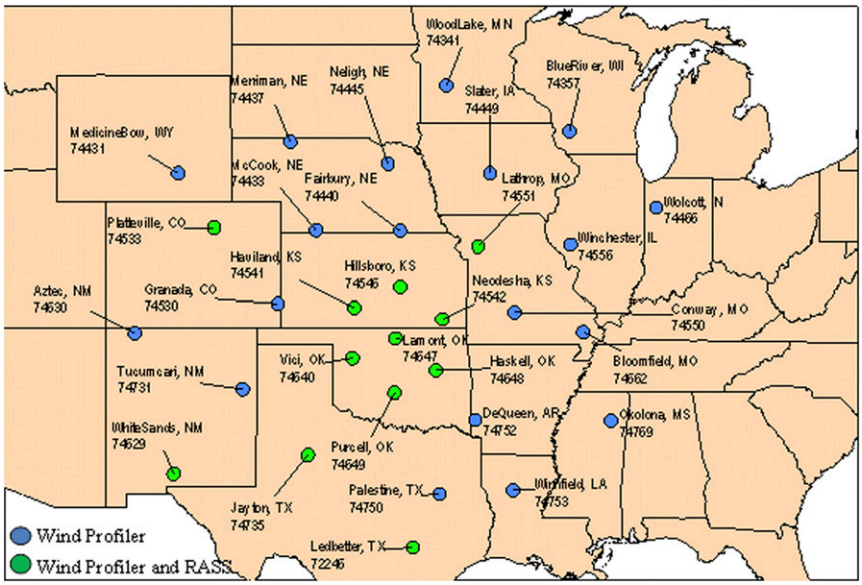

FIG. 1. Map of NPN sites used in this study. Filled blue circles indicate WP stations and filled green circles identify wind profiler stations that also have RASS.

In the frequency range at which the profilers transmit, the signal is undergoing Bragg scatter, essentially responding to changes in atmospheric density. These density changes are caused by changes in water vapor, temperature, aerosol, or hydrometeor content. Changes in atmospheric aerosol, water vapor, or temperature with height are sharpest near the top of the planetary boundary layer, and so the wind profiler data may be used to detect boundary layer height.

The limitations of wind profiler data were addressed in OFCM (1998). UHF wind profilers are limited in that they must assume a local horizontal uniformity. An example of problems related to inhomogeneous terrain will be shown in section 4. Two other issues related to wind profiler data are contamination from migrating birds and insect swarms, which may flood the signal return. In addition, because of potential interference with the receivers on the six polar-orbiting satellites, the wind profiler's transmitter shuts down for 6 min during satellite overpasses. This occurs about 7 times daily (varying between 4 and 10 times) for each site in the network. One of the most significant limitations for the use of wind profiler data to compute PBL heights is the inability to gather data between the surface and 500 m, and therefore it precludes the ability to measure nocturnal PBL heights. Despite these limitations, wind profiler data may be used to provide long-term hourly time series of daytime PBL heights.

b. *Additional data for the algorithm and its validation*

Data at each NPN station included an additional set of files containing surface variables. The surface files contain hourly surface temperature, mean sea level pressure, wind direction, relative humidity, dry-bulb temperature, and rainfall. Virtual potential temperature at the surface was computed from the relative humidity and dry-bulb temperature. The saturation vapor pressure was computed based on WMO (2008).

Twelve of the wind profiler sites are equipped with radio acoustic sounding system (RASS) instruments, seven of which have archived data records that are used here. RASS-based profiles of virtual temperature are provided in the NPN archive, and are used in this study along with the retrieved wind profiles from the profilers to estimate a Richardson number–based PBL height, which will be described in the next section. The RASS virtual temperature retrieval algorithm is based on the sensitivity of the speed of sound to temperature. The RASS instruments emit acoustic energy and measure the speed of the sound waves as they propagate up through the atmosphere (Singal and Goel 1997).

The analysis of PBL heights includes distinctions between clear and cloudy days. Cloud cover at the NPN sites was determined based on data from the International Satellite Cloud Climatology Project (ISCCP) D1 data product (Rossow et al. 1996), which is a global gridded cloud product with a resolution of 290 km^2 at 3-h intervals. For this study we used the cloud cover percentages (number of cloudy pixels/total number of pixels times 100) for the grid square closest to a given NPN station. ISCCP data were chosen for the determination of cloud cover due to the availability of high-temporal-resolution data during the time span of NPN data.

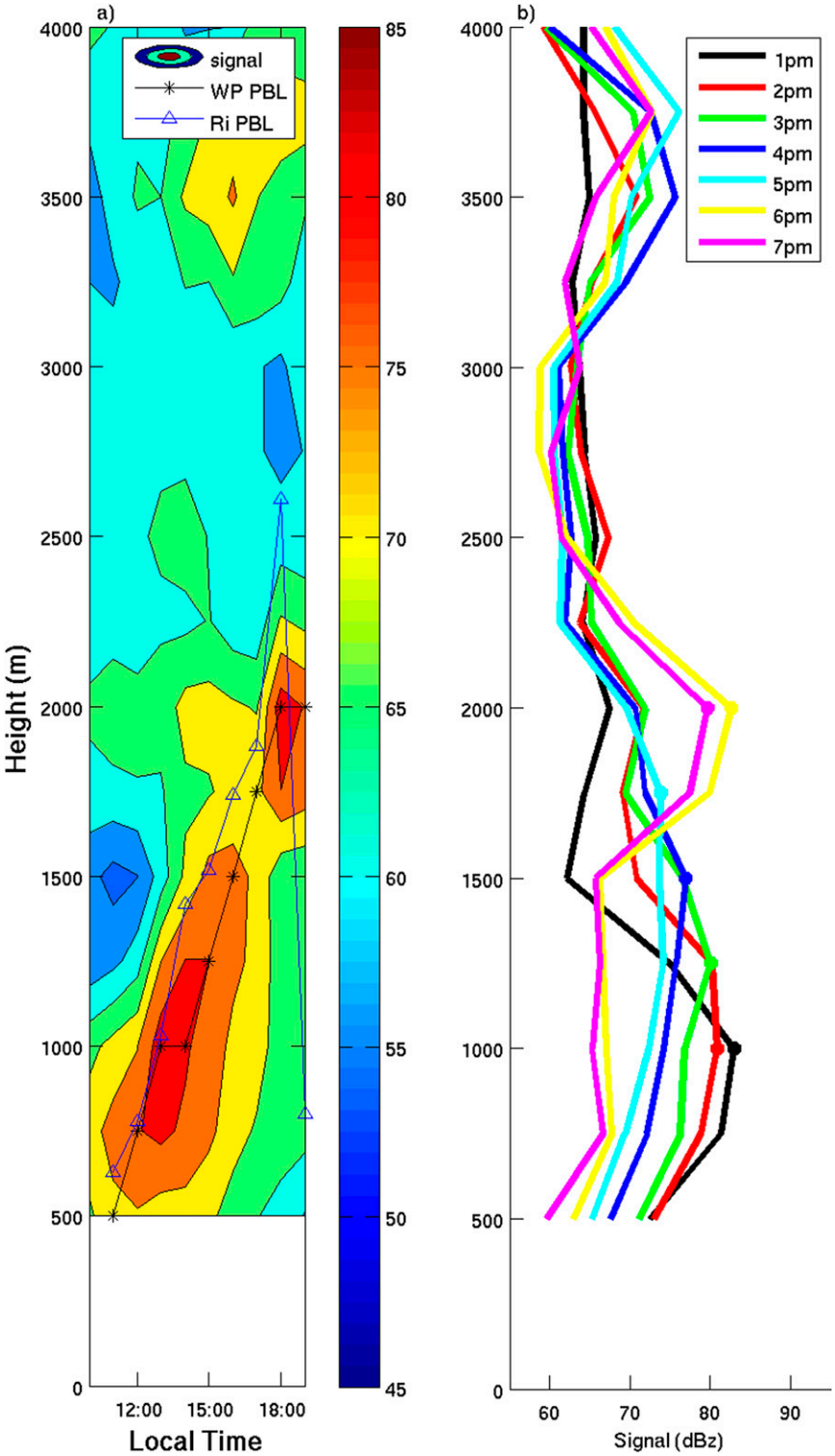

FIG. 2. Example of diurnal evolution of PBL height from station 74541. (a) Shading is backscatter signal strength (dBZ), blue triangles are estimates of PBL height computed using the Richardson number–based method, and the black asterisks are the PBL heights from the WP algorithm. (b) Vertical profiles of the WP backscatter (dBZ) up to a height of 4000 m for every hour starting at 1300 LT. WP PBL heights in each profile are marked with a filled circle.

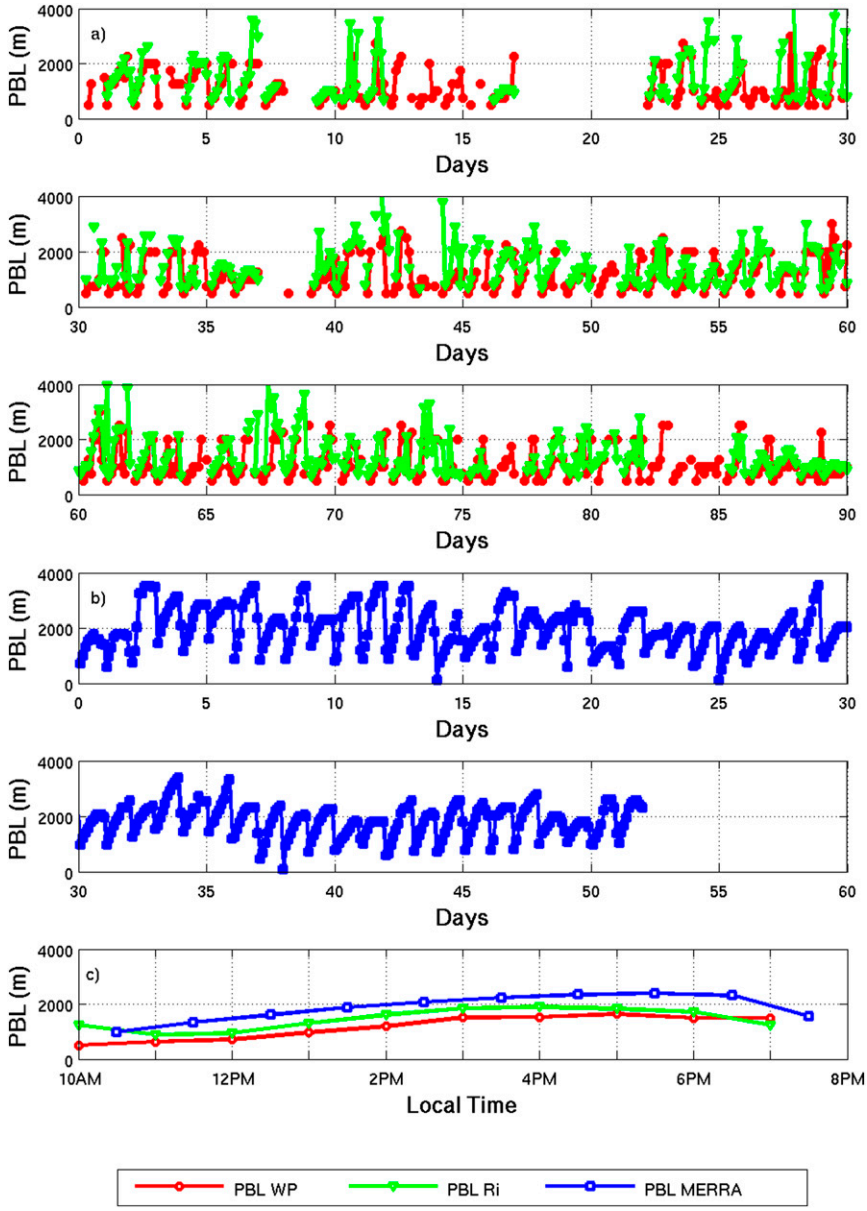

FIG. 3. Example of a discontinuous time series of PBL heights (m) at station 74541, from (a) the WP algorithm and the Richardson number–based algorithm and (b) from MERRA. (c) Climatological diurnal cycle for all three estimates.

Reanalysis estimates of PBL height for comparison with wind profiler estimates were obtained from the Modern-Era Retrospective Analysis for Research and Applications (MERRA; Rienecker et al. 2011) two-dimensional surface turbulent flux dataset (tavg1_2d_flx_Nx). Files were obtained from the NASA Goddard Modeling and Assimilation Data and Information Services Center (MDISC; http://disc.sci.gsfc.nasa.gov/mdisc/data-holdings). These data are available hourly, at a spatial resolution of 0.667° in longitude and 0.5° in latitude. MERRA PBL heights are diagnosed by the turbulence parameterization in the underlying atmospheric general circulation model based on the eddy diffusivity coefficient for heat. The PBL height is diagnosed as the level at which the coefficients drop below a value of $2\,\mathrm{m\,s^{-2}}$. Clear-sky daily maximum MERRA PBL heights were shown to be generally lower than satellite-based *Cloud–Aerosol Lidar and Infrared Pathfinder Satellite Observations* (*CALIPSO*) estimates over tropical oceans (Jordan et al. 2010) and are shown

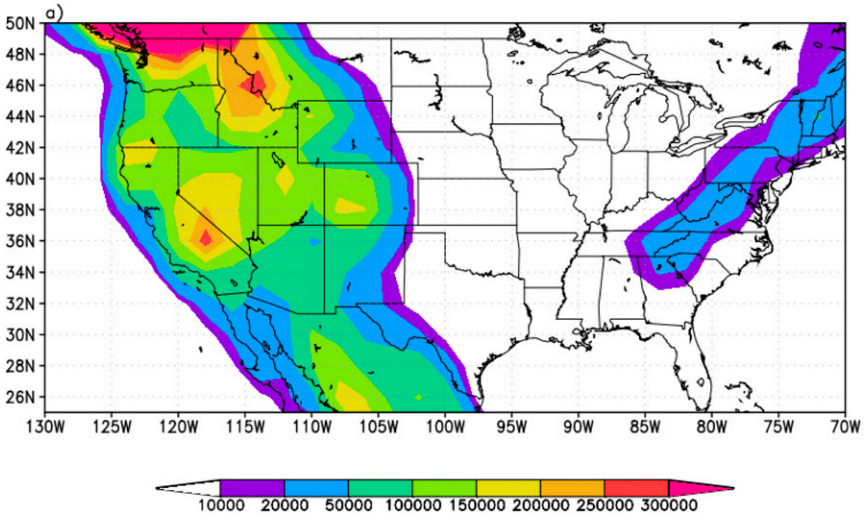

FIG. 4. (a) Variance of topographic height at scales < 3 km (m^2). (b) Diurnal evolution of PBL height from station 74629. Shading is backscatter signal strength (dBZ), and black asterisks are the PBL heights from the WP algorithm. (c) Vertical profiles of the WP backscatter for the same location as in (b) up to a height of 4000 m for every hour starting at 1300 LT.

to be relatively consistent with *CALIPSO* over land (McGrath-Spangler and Denning 2012).

3. Estimation of PBL height

The algorithm for estimating PBL heights from wind profiler (WP) data was initially developed for clear-sky conditions and refined using data from a station for which RASS temperature measurements were available. Cloud cover was determined using the ISCCP data at the grid point containing the station under examination, and clear days were selected based on the condition that at 1000, 1300, and 1600 LT, there was 0% cloud cover. The initial step of the algorithm, and a unique feature of the algorithm developed in this study, consists of determining the time of day at which the PBL rises from its nocturnal value into the range of instrument detection at 500 m above the ground. This step of the algorithm fills the role served by more complicated algorithm details (e.g., Bianco et al. 2008) or specific limits (Compton et al. 2013) that are present in many algorithms to deal with the noisy morning SNR profiles that are measured when the PBL height is below instrument range. The underlying assumption for the algorithm developed here, as well as most lidar or wind profiler PBL height algorithms, is that the gradients of moisture, hydrometeors, or particles at or near the PBL height will be manifest as maxima in the signal backscatter at the detector. The time at which the PBL height emerges into the instrument's range is therefore the time at which the signal backscatter at the 500-m level is at its daily maximum. Once this "emergence time" is established, the vertical profile of signal backscatter is examined at each subsequent hour to determine the WP PBL height. If only one local maximum exists for a given hour's profile, then the PBL height is assigned to the height of that maximum. If multiple local maxima exist, as was the case for the vast majority of profiles examined, then the standard deviation of the column backscatter (up to the level of the largest local maximum) is used to choose which among the local maxima is the "true maximum," and the PBL height is assigned to the height of that true maximum. Starting from the lowest height at which a local signal maximum exists, each maximum is evaluated against the local minimum above it using the column standard deviation to determine whether it is a true maximum or a small "wiggle" in the profile and therefore not the PBL. Any signal maximum value not larger than the minimum above it by more than one standard deviation is deemed a wiggle and the process of evaluating local maxima proceeds upward in the column. If a true maximum is found, then the PBL height is assigned to the height of that maximum; if none is found, then the algorithm does not return a value for the WP PBL height.

PBL heights were also estimated at the NPN stations with RASS data (seven of the stations) using the retrieved virtual temperature profiles and the retrieved wind profiles in the NPN archive. The temperature and wind fields were used to compute a bulk Richardson

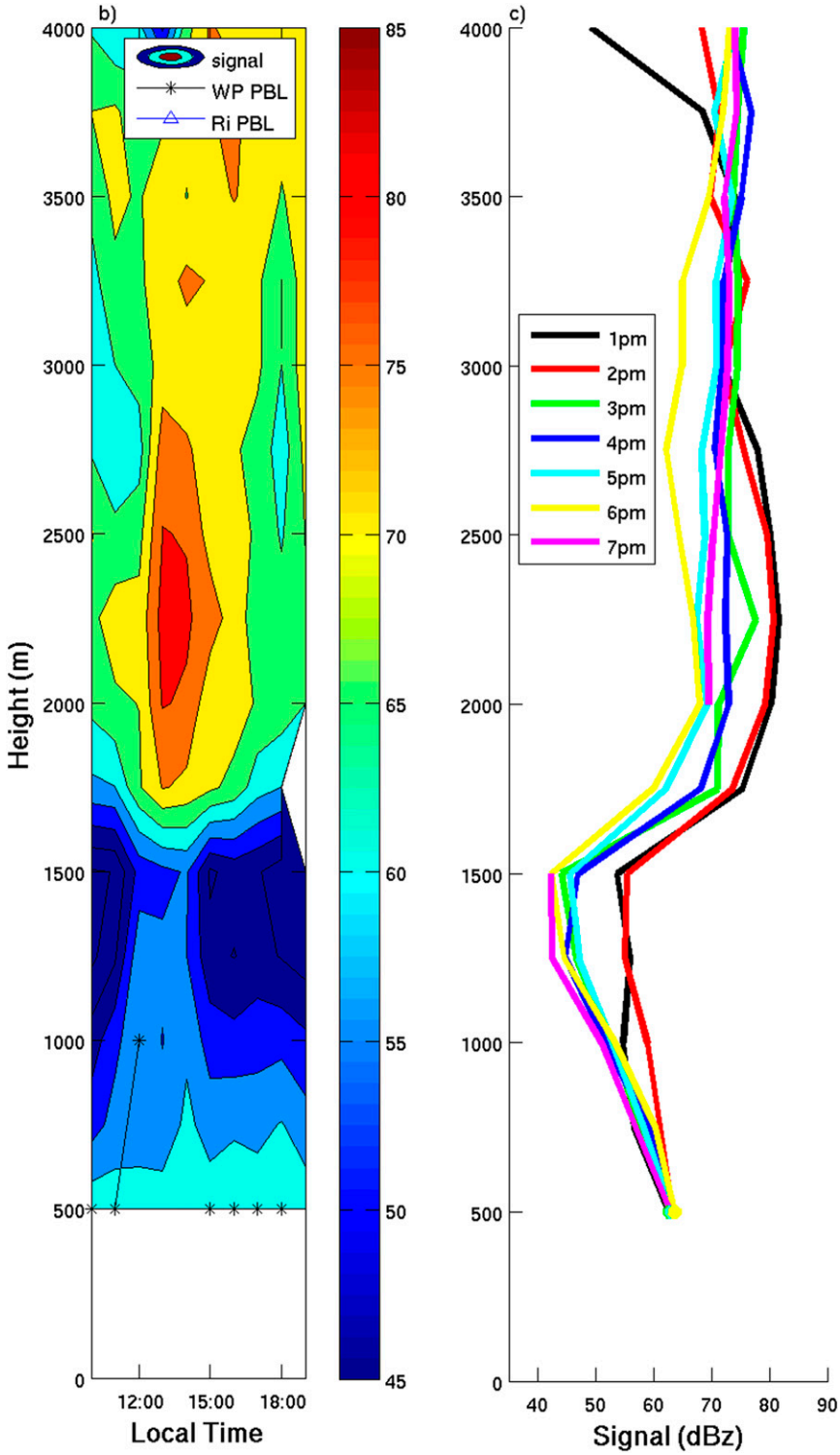

FIG. 4. (*Continued*)

number (Ri_b)-based PBL height estimate after Seidel et al. (2010). The Ri_b used is given by

$$\mathrm{Ri}_b = \frac{\left(\frac{g}{\theta_{v,s}}\right)(\theta_{v,z} - \theta_{v,s})(z - z_s)}{u_z^2 + v_z^2},$$

where g is gravity, θ_v is the virtual potential temperature, u and v are the horizontal wind components, and z is height. The subscript s denotes the surface, and the surface winds are assumed zero. This bulk Richardson number is evaluated based on differences between the surface and successively higher heights, assuming that the surface layer is unstable, and the PBL top is identified as the level at which Ri_b exceeds a critical value of 0.25. The choice of 0.25 as the critical Richardson number for this study was chosen for consistency with the study of Seidel et al. (2010). PBL height values using a critical Richardson number of 0.20 were also obtained and were found to be statistically indistinguishable from the PBL heights computed using a threshold of 0.25. This additional quasi-independent estimate of PBL height was used for validation purposes during the algorithm development and for comparison afterward. Seidel at al. (2010) found that this Ri_b PBL height algorithm outperformed a θ_v gradient algorithm such as the one used in Bianco and Wilczak (2002) for validation.

An example of the correspondence between the PBL height selected by the WP algorithm and the vertical profiles of the wind profiler backscatter is shown in Fig. 2, based on data for station 74541 (Havilland, Kansas) on 4 July 2003. The collocation of the maximum in the contours of signal strength with the PBL height (black stars) at each time of day is depicted in Fig. 2a and demonstrates the general behavior of the algorithm developed here. In this example, the PBL height rises above 500 m in the late morning; it reaches the daytime maximum of approximately 2000 m in the late afternoon and remains there until 1900 LT. The existence of elevated PBL heights late in the afternoon is to be expected based on the response of the wind profiler to aerosol–hydrometeor loads, which on a clear day essentially measures the height of an "aerosol boundary layer." Similar behavior of the diurnal cycle was found by Angevine et al. (1994) using wind profiler SNR at a location in Alabama; by Cohn and Angevine (2000) at a location near Champagne, Illinois; and by Lewis et al. (2013) at a location in Beltsville. Figure 2b shows the vertical profiles of the wind profiler backscatter up to a height of 4000 m for every hour starting at 1300 LT. Figure 2b shows clearly that at each time of day there are multiple maxima in the profiles and that the ability to distinguish between them is an important element of the algorithm.

4. Results and discussion

The WP PBL height algorithm was applied to all available data from the stations shown in Fig. 1, for June–August of 2000–05. Only data with a "0" quality control flag were considered. Comparisons were made to PBL height estimates obtained using the Richardson number–based calculation described in section 3 and to the PBL heights from MERRA, which are model-based estimates using observationally constrained atmospheric profiles. The focus of the results presented here is on mean diurnal cycles for each station and for each PBL height estimate (WP, Ri_b, and MERRA) under both clear and mostly cloudy conditions. The mean diurnal cycle is computed as the average at each time of day over all clear (or cloudy) days in the study's time span. The time span was adequate to provide at least 10 days in each category for the calculation of the mean diurnal cycle. Statistical analysis of the results is presented using correlations among the time series of the difference estimates, as the variability is too large and the sample size too small for comparisons based on Student's t tests.

An example of a PBL height time series for all the clear days at the Havilland station during the study period is shown in Fig. 3. The time series curves in Figs. 3a and 3b represent the PBL evolution over a series of juxtaposed 10-h segments from 1000 to 1900 LT on all clear days for the WP, Ri_b, and MERRA estimates. The station-derived (Fig. 3a) clear-sky determination is based on ISCCP data, and the MERRA determination (Fig. 3b) uses its own estimate of cloud fraction and thus is represented by a different sample of days. The daily maxima of the WP, Ri_b, and MERRA PBL heights range between 2000 and 3000 m, with MERRA PBL heights occasionally reaching values up to 3500 m and Ri_b PBL heights reaching values up to 4000 m. The clear-day mean diurnal cycle for the station in Figs. 3a and 3b is shown in Fig. 3c. In this example, the mean diurnal cycle of the all three PBL height estimates are qualitatively similar in character throughout the day.

As was mentioned in section 2a, inhomogeneous terrain surrounding wind profiler stations may present problems for use of wind profiler data. A map of the terrain variance at scales less than 3 km in the study region (Fig. 4a) indicates that New Mexico, Wyoming, and Colorado are characterized by large topographic variations that may interfere with the use of wind profiler backscatter data to determine PBL heights. An

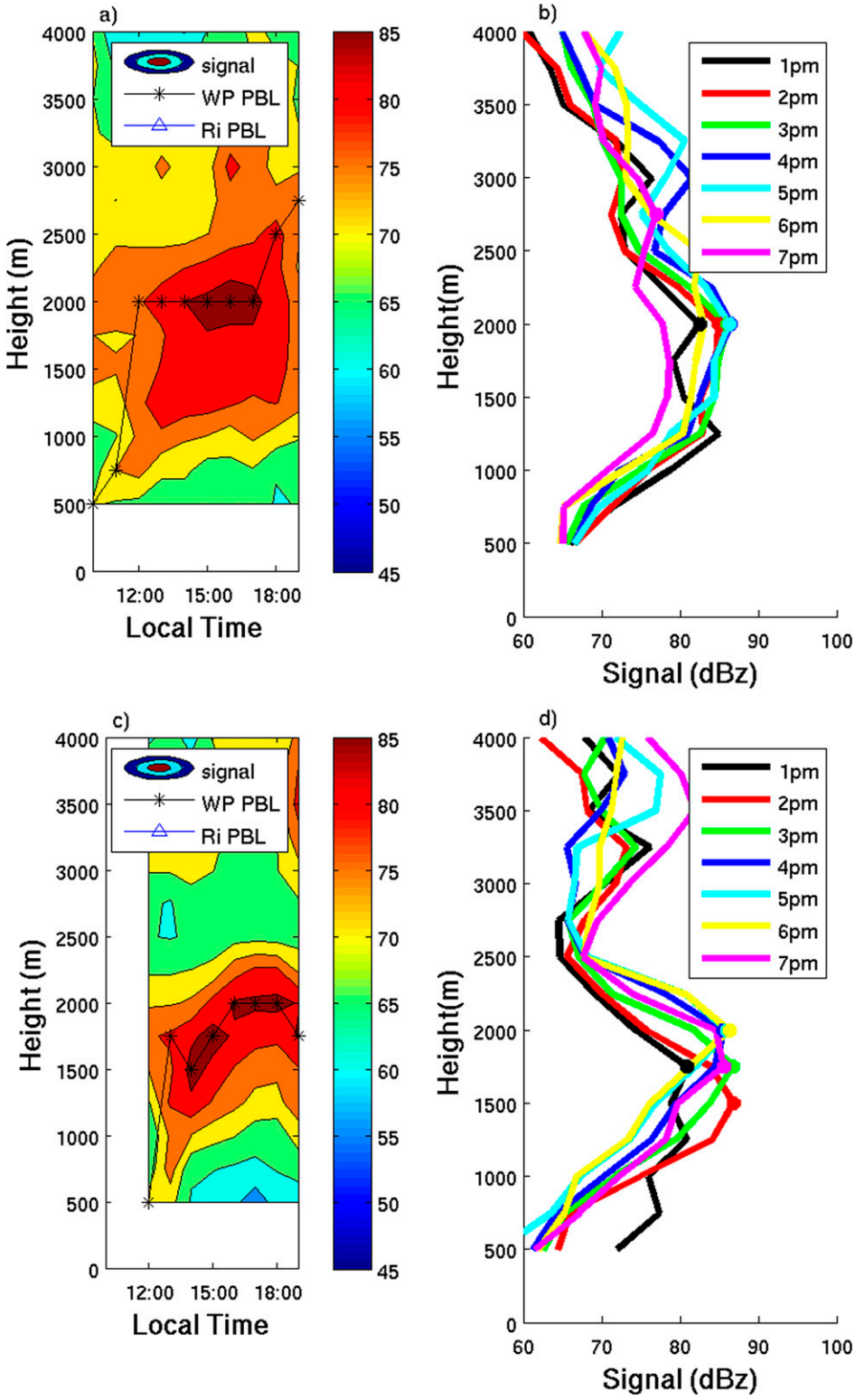

FIG. 5. Examples of diurnal evolution of PBL height from station 74551. (a) Sample clear-sky day's data. Shading is backscatter signal strength (dBZ), black asterisks are the PBL heights from the WP algorithm. (b) Vertical profiles of the WP backscatter up to a height of 4000 m for every hour starting at 1300 LT. (c),(d) As in (a),(b), but for a cloudy-sky day, respectively.

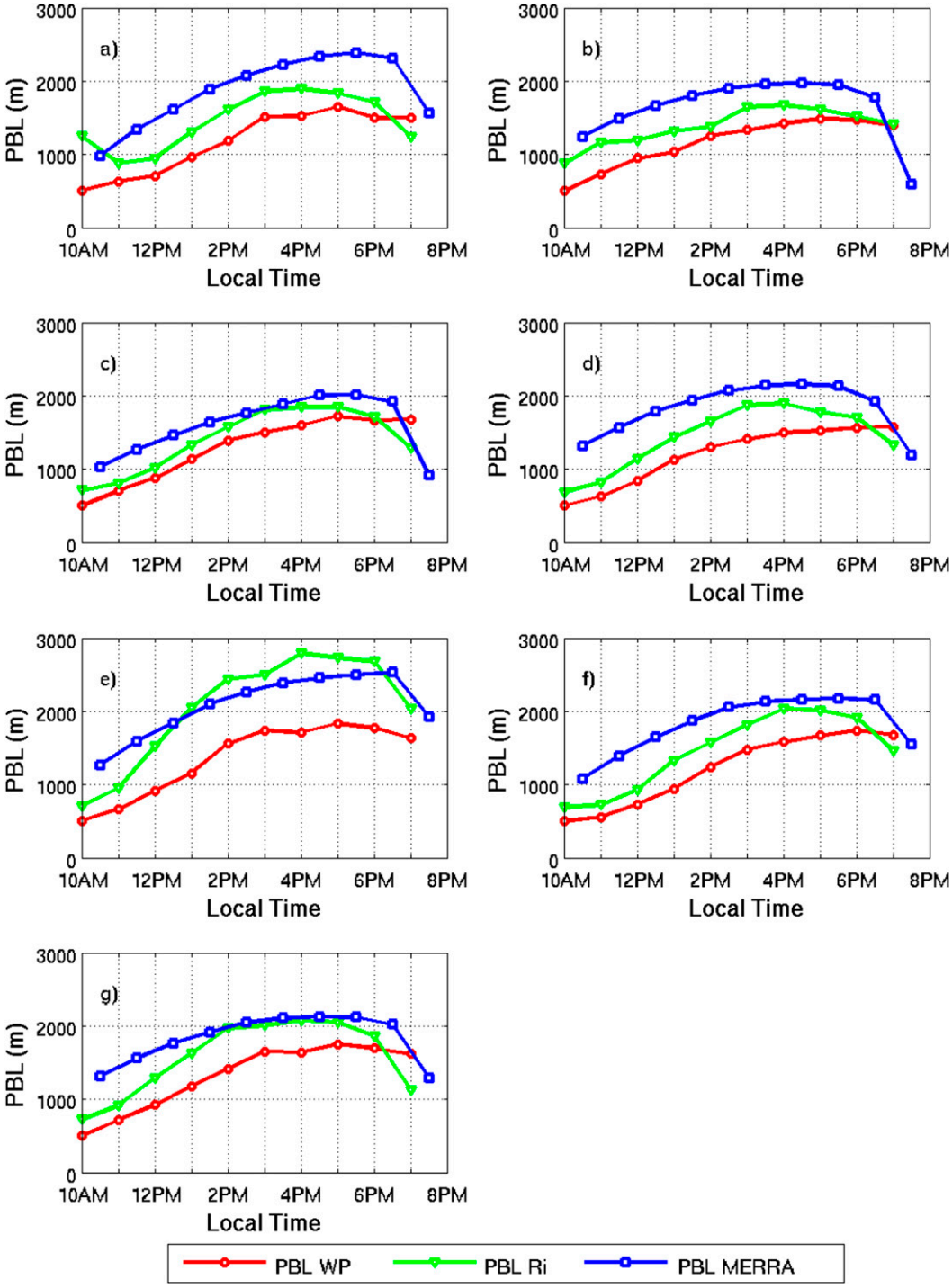

FIG. 6. Climatological diurnal cycles of WP (red), Richardson number (green) and MERRA (blue) estimates of PBL height (m) under clear-sky conditions for the seven stations with RASS. Station numbers correspond to the labels in Fig. 1: (a) station 74541, (b) station 74542, (c) station 74546, (d) station 74648, (e) station 74735, (f) station 74640, and (g) station 74649.

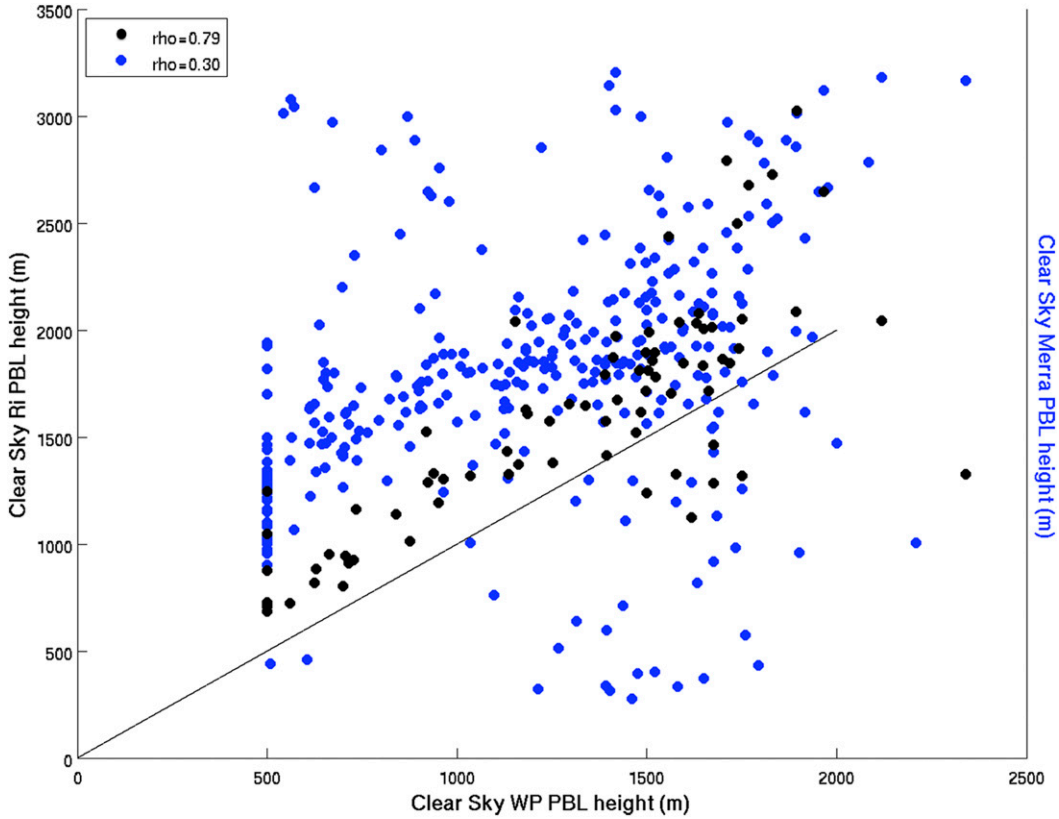

FIG. 7. Scatter diagram of clear-sky WP vs Richardson number–based seasonal mean PBL heights (m; black points) and WP vs MERRA PBL heights (m; blue points). The legend includes the correlation coefficient of the two time series (RHO).

example of the typical behavior of the WP algorithm over station 74629 in White Sands, New Mexico, is shown in Figs. 4b and 4c. The signal backscatter decreases with height up to approximately 1750 m at all times of the day, and then above that level it increases to a local maximum at approximately 2250 m. This behavior makes it difficult to subjectively determine a PBL height "by eye," and in practice the step in the algorithm that searches for a PBL emergence time fails. This behavior is typical for the stations in New Mexico, Colorado, and Wyoming, and for this reason they are removed from the analysis of the WP PBL heights to be presented in the remainder of section 4.

Another type of issue with the WP PBL height algorithm at particular stations is demonstrated in Fig. 5, in which the signal backscatter (Figs. 5a and 5c) and line plots at two individual times (Figs. 5b and 5d) are shown from station 74551 in Lathrop, Missouri, on a clear day, 21 July 2002, and on a cloudy day, 9 August 2002. In the clear-day example shown here, the backscatter signal maximum occurs at a level that grows (unreasonably) rapidly in the morning hours, from 750 to 2000 m in the span of an hour, remains constant at 2000 m at all times of day after 1200 LT, and rises to 2700 m at 1900 LT. In the cloudy-sky example, the rapid growth is from 500 to 1750 m in the span of an hour, rising to 2000 m soon afterward, and remaining at 2000 m throughout the day. This pattern of behavior occurs on many clear and cloudy days during the study period, at the station depicted in Fig. 5, and at the nearby station in Wolcott, Indiana (station 74466), and determines the behavior of the mean WP PBL height diurnal cycle under clear and cloudy conditions at those two stations. An aerosol layer advected into the range of the station could potentially cause such behavior, but because of the unusual pattern of signal backscatter, these two stations are also excluded from the analysis in this section.

a. *Clear-sky PBL heights*

The mean diurnal cycles under clear-sky conditions for the seven stations with RASS data are shown in Fig. 6. In general throughout the morning and the early afternoon, the estimates of PBL height from the WP algorithm (red) are lower than the PBL heights from the Ri_b algorithm (green) by up to 500 m, which in turn lie below the MERRA PBL heights (blue) by the same

amount. In the early evening the WP PBL heights are below the MERRA values and comparable to the Ri_b PBL values, and in the late evening the Ri_b and MERRA heights drop and the WP PBL heights generally remain elevated. This behavior of the WP PBL heights in the evening is expected based on the discussion in section 3 of the sensitivity of wind profiler backscatter to changes in density. The rate of morning PBL height growth is similar among all three PBL height estimates. This characterization of the relationship between the clear-sky mean diurnal cycles of the WP and MERRA PBL heights also holds for the stations without RASS instruments.

The seasonal mean clear-sky WP PBL heights at station 74546 (Hillsboro, Kansas; Fig. 6c) are comparable in magnitude and diurnal cycle to the PBL height estimates of Liu and Liang (2010) using radiosonde profiles at the nearby Atmospheric Radiation Measurement Program Southern Great Plains (ARM SGP) site. According to the authors, the median radiosonde-derived PBL heights during June–August reach a daily maximum of approximately 1700 m just after 1500 LT, remain elevated until 1800 LT, and then drop quickly. The WP PBL heights seen in Fig. 6c also reach a daily maximum of approximately 1700 m at approximately 1600 LT and remain elevated for the remainder of the day.

A statistical summary of the clear-sky PBL heights and the relationships among the different estimates of the seasonal mean behavior is depicted in the scatter diagram of Fig. 7. Each point in the scatter diagram represents either a comparison between the WP seasonal mean PBL height and the seasonal mean Ri_b (black) or the MERRA (blue) PBL height at a particular time of day at a particular station. The correlation coefficient describing the linear correlation between the WP and Ri_b PBL heights is 0.79, demonstrating that although there is an offset between the two estimates (black dots are usually above the line showing perfect correspondence), the variations in the two series are well correlated. The correlation coefficient between the WP and MERRA values is 0.30, showing less of a correspondence due to the presence of a cluster of WP PBL heights near 1500 m, where the MERRA heights are closer to 500–1000 m. These points are generally late in the day (see Fig. 6).

Figure 8 shows the geographical distribution of the maximum of the mean diurnal cycle of the clear-sky PBL heights from the WP and MERRA estimates at all the wind profiler stations in the study region. The WP PBL heights are highest at the stations located to the west and south and decrease eastward and northward. This pattern generally follows the expected dependence of PBL height on surface temperature and moisture, where the higher PBL heights are found in the warmer and drier areas to the west and south, and lower PBL heights are found in the cooler and moister areas to the north and east. The pattern of MERRA PBL heights is quite different, with large PBL heights in the center of the region. In general, as was seen in Fig. 6 at the RASS stations and in the scatter diagram in Fig. 7, MERRA PBL heights are higher than WP PBL heights. The warm summertime bias in MERRA surface temperatures in the Great Plains (Bosilovich 2013) would suggest that MERRA PBL heights are biased high. The warm MERRA surface temperatures along with the agreement between WP PBL heights and the ARM SGP estimates of Liu and Liang (2010) support the credibility of the WP PBL height estimates. The daily maximum PBL height at the station in Winchester, Illinois (station 74556), is approximately 1500 m in both the WP and MERRA estimates. These values are in good agreement with the daily maximum PBL height estimates under clear-sky conditions obtained by Angevine et al. (1998) and by Cohn and Angevine (2000) as part of the Flatlands 1995 and 1996 experiments in

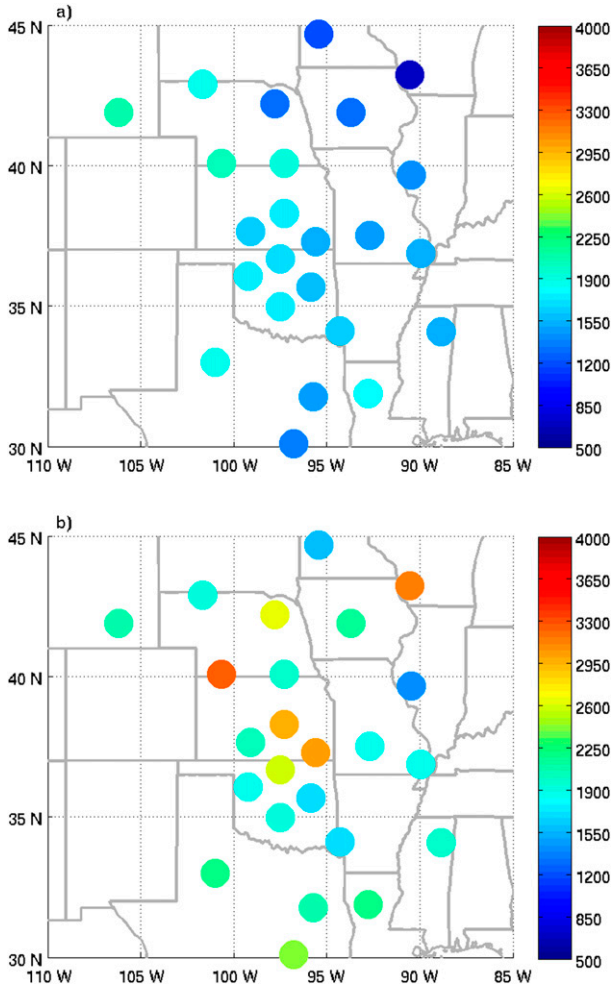

FIG. 8. Geographical distribution of daily maximum PBL height (m) under clear-sky conditions from (a) WP estimate and (b) MERRA estimate.

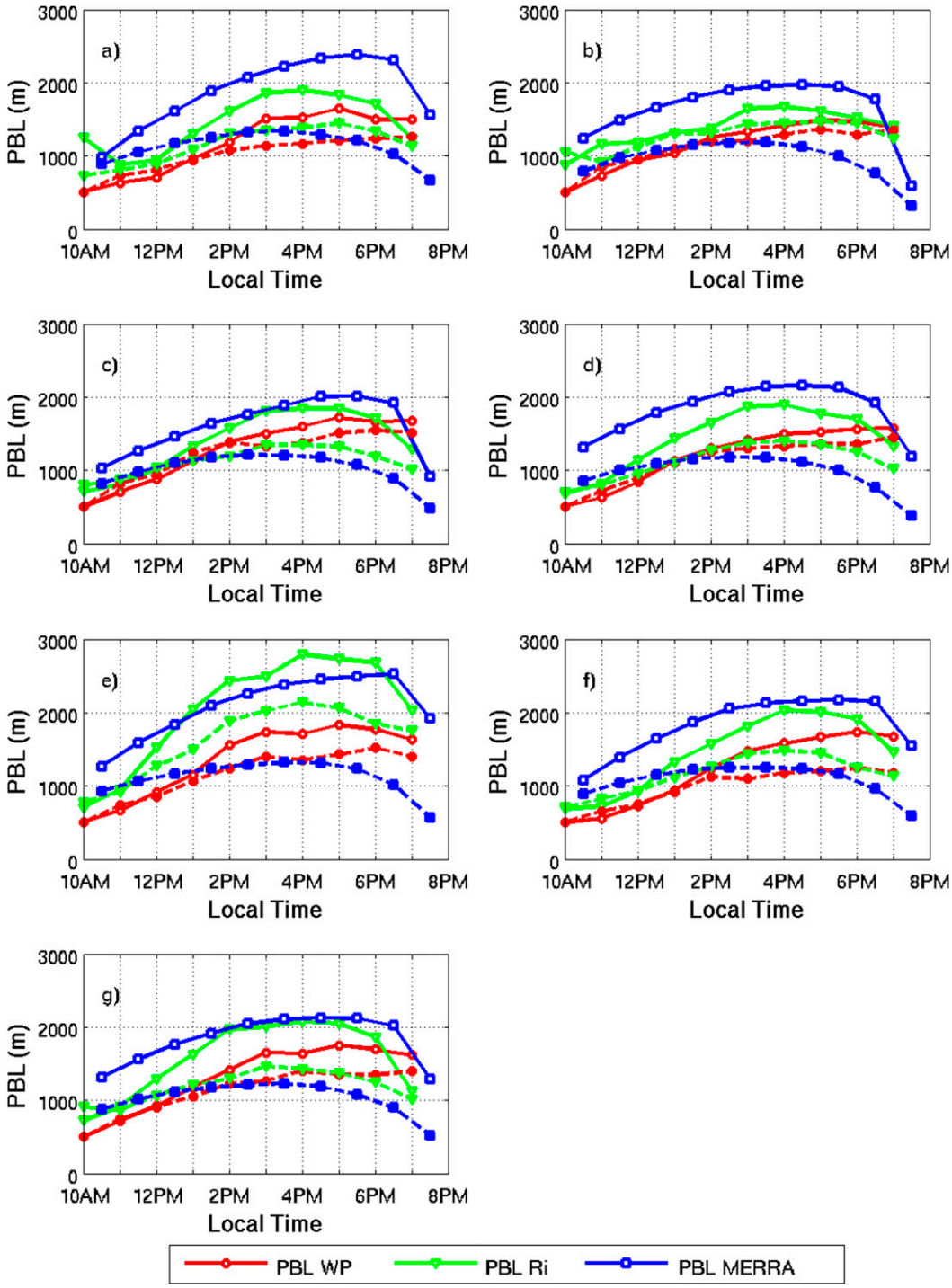

FIG. 9. As in Fig. 6, but for >50% cloud cover (dashed lines) in addition to under clear-skies (solid lines).

nearby Champagne. The daily maximum values at Lamont, Oklahoma (station 74647), are also in good agreement with the wind profiler and radiosonde PBL heights computed by Simpson et al. (2007) during selected days in July 2003 over Oklahoma City, Oklahoma.

b. *PBL heights under cloudy-sky conditions*

Algorithms to estimate PBL heights from lidar or wind profiler data have generally been restricted to clear-sky conditions (Angevine et al. 1994; Bianco and

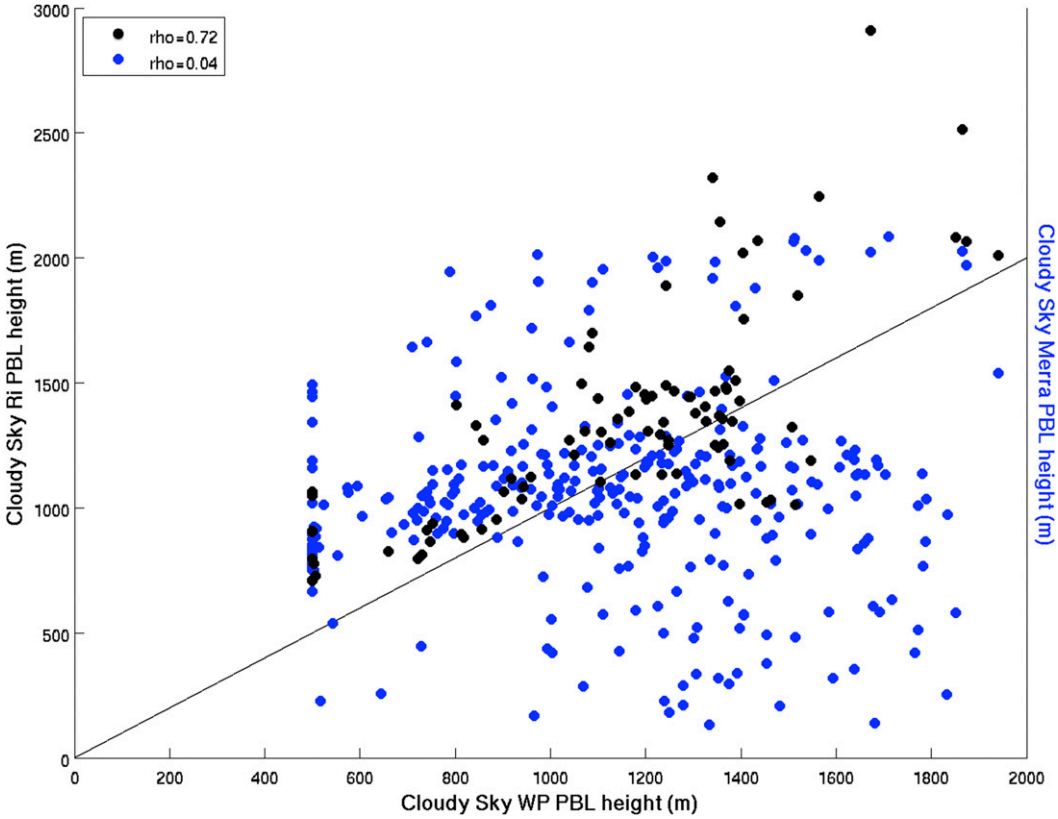

FIG. 10. As in Fig. 7, but for mostly cloudy-sky wind conditions.

Wilczak 2002; Lewis et al. 2013), or have attempted to estimate PBL heights in cloudy-sky conditions with limited success (Bianco et al. 2008). The present WP PBL height algorithm was applied on all the mostly cloudy-sky days (cloud cover > 50%) during the study period at each station. The partially cloudy-sky (cloud cover < 50%) PBL heights are not considered here because the results were unrealistic and we consider the algorithm unreliable for partially cloudy-sky conditions.

The mean diurnal cycles under mostly cloudy-sky (>50% cloud cover) conditions for the seven stations with RASS data are shown in Fig. 9 alongside the clear-sky PBL heights shown in Fig. 6. At most stations, the cloudy-sky PBL heights from WP, Ri_b, and MERRA are in close agreement from the morning until approximately 1400 LT. After this time, the MERRA cloudy-sky PBL heights drop, while the WP PBL heights remain aloft and the Ri_b PBL heights vary in behavior from station to station. The cloudy-sky PBL heights are expected to be lower than the clear-sky values due to the decreased net radiation at the surface under cloudy-sky conditions, and this is seen in all three PBL height estimates. The MERRA PBL heights exhibit the largest clear-sky minus cloudy-sky difference throughout the day, with values up to 1000 m (consistent with a possible overestimate of MERRA clear-sky PBL heights); the Ri_b PBL height clear-sky minus cloudy-sky differences generally vary between 500 and 750 m; and the WP PBL height difference is smallest, with values generally near 0 m in the morning and closer to 250 m after 1400 LT.

The statistical summary of the mostly cloudy-sky PBL heights and the relationships among the different estimates of the seasonal mean behavior is shown in Fig. 10. As in Fig. 7, each point in the scatter diagram represents a comparison between the WP seasonal mean PBL height and the seasonal mean Ri_b (black) or MERRA (blue) PBL height at a particular time of day at a particular station. The correlation coefficient describing the linear correlation between the WP and Ri_b PBL heights is 0.72, demonstrating, as for the clear-sky conditions, that although there is an offset between the two estimates (black dots are usually above the line showing perfect correspondence), the variations in the two series are well correlated. The correlation coefficient between the WP and MERRA values is 0.04, showing that there is no correspondence. The lack of correlation is associated with the times of day after 1400 LT, where the disagreement between WP and MERRA PBL heights was largest, as was shown in Fig. 9.

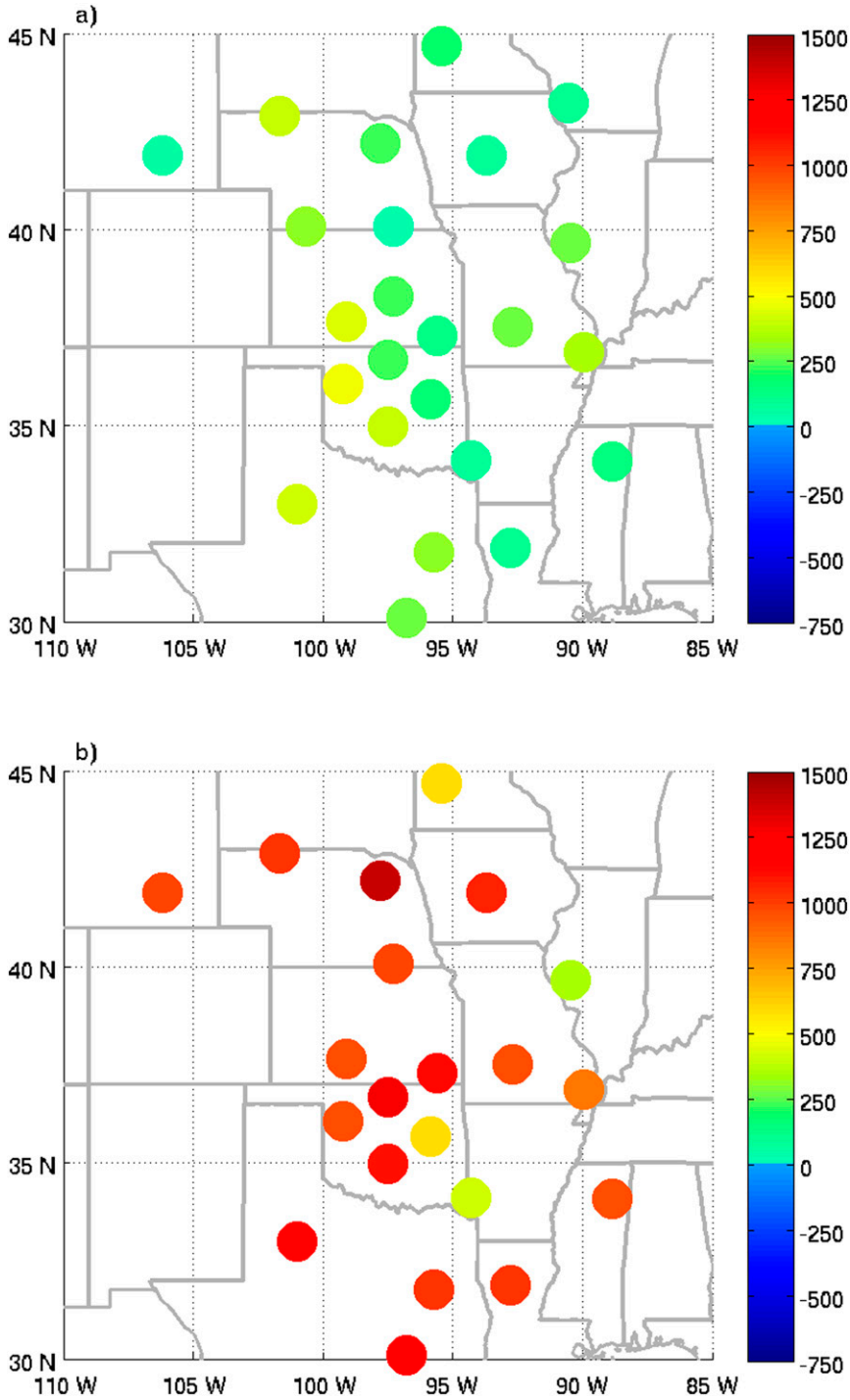

FIG. 11. As in Fig. 8, but for clear-sky PBL height minus daily maximum PBL height (m).

Figure 11 shows the geographical distribution of the daily maximum of the clear minus cloudy-sky PBL height difference from the WP and MERRA estimates at the wind profiler stations in the study region. The behavior at all the stations is qualitatively the same as the behavior at the stations with RASS shown in Fig. 9; that is, the MERRA clear-cloudy PBL height difference is generally quite a bit larger (by approximately 750 m) than the WP difference. The WP clear–cloudy difference also shows the geographic pattern seen in the

clear-sky PBL heights, with a larger clear–cloudy difference in the western areas of the study region and smaller difference in the eastern areas. This pattern stems from a more geographically uniform cloudy-sky PBL height, suggesting that the cloudy-sky PBL height is less sensitive to the surface temperature and moisture than the clear-sky PBL height. The MERRA PBL clear–cloudy PBL height difference shows little of this geographical pattern.

5. Summary and conclusions

An algorithm was developed to compute planetary boundary layer (PBL) heights using wind profiler backscatter signal data archived by the NOAA wind profiler network. Data for this study were from June through August of 2000–05, and the study area is the central United States. The wind profiler (WP) PBL height algorithm estimates the ''emergence time'' of the PBL height into the range detectable by the instrument and selects the appropriate local maximum backscatter value in each column to designate as the PBL height. The need for an entire day's worth of backscatter data to determine the emergence time precludes the use of this algorithm for operational PBL height forecasts. WP PBL heights were evaluated under clear- and cloudy-sky conditions relative to PBL height estimates from the MERRA reanalysis and from a quasi-independent estimate based on RASS temperature profiles available at a subset of the NOAA wind profiler stations using a bulk Richardson number (Ri_b) algorithm. At some stations the variation with height of the signal backscatter data does not reflect the PBL discontinuity, because of topographic variations (the six stations in Wyoming, Colorado, and New Mexico) or because of the possible presence of aerosol layers advected from nearby (the stations at Lathrop and at Wolcott), and these stations were excluded from the study. The algorithm presented here is characterized by its simplicity, in that it requires few steps. In addition, unlike many previous studies, the validation of the present algorithm was comprehensive, in that the WP PBL heights were evaluated over a long period of time and over a wide geographic range. The robustness is largely due to the simplicity.

Clear-sky mean diurnal cycles typically show the PBL emergence into instrument range occurring at approximately 1000–1100 LT. The WP PBL height increases in the morning and early afternoon hours until it reaches its daily maximum at approximately 1600 LT and levels off afterward. The WP PBL heights agree with Ri_b-based PBL heights at RASS stations in the morning, are lower by approximately 250 m than the Ri_b PBL heights in the afternoon, and are lower in general than the MERRA PBL heights by up to 1000 m in the early afternoon. The WP and Ri_b PBL heights are well correlated, and the WP and MERRA PBL heights are less so. The geographical distribution of daily maximum WP PBL heights follows the expected variation with temperature and moisture, where higher PBL heights occur over warmer and drier terrain—a distribution not reflected in the MERRA PBL heights.

Cloudy-sky WP PBL heights show a similar general diurnal cycle as the clear-sky heights in terms of emergence time and time of daily maximum, and are generally lower than clear-sky PBL heights as expected. The cloudy-sky WP PBL heights are comparable to the other estimates until 1400 LT, when they are higher than the MERRA PBL heights later in the afternoon. The clear-cloudy PBL height differences are smaller for the WP PBL heights than for either the Ri_b (by up to 250 m) or the MERRA PBL heights (by up to 500 m), possibly reflecting an overestimate of WP cloudy-sky PBL heights and an overestimate of MERRA clear-sky PBL heights. As was the case for the clear-sky PBL heights, the WP and Ri_b PBL heights are well correlated, but for cloudy conditions the WP and MERRA PBL heights are uncorrelated. The geographical distribution of the clear–cloudy difference in daily maximum PBL heights is smoother than the clear-sky PBL height distribution, but it also reflects the variations in temperature and moisture, where larger clear–cloudy differences occur in warmer and drier areas.

The present study has shown that existing data archives from the NOAA Profiler Network (NPN) can be used to provide reliable estimates of hourly PBL heights under clear-sky and mostly cloudy-sky conditions at an extensive set of locations in the central United States. Signal backscatter data are available from the NPN throughout the year, and for varying time periods at different stations. Future work will extend the temporal scope of this study to include the entire time span for each station in the wind profiler network archive and to include the analysis of annual cycles and interannual variability.

REFERENCES

Angevine, W. M., A. B. White, and S. K. Avery, 1994: Boundary-layer depth and entrainment zone characterization with a boundary-layer profiler. *Bound.-Layer Meteor.,* **68,** 375–385, doi:10.1007/BF00706797.

——, A. W. Grimsdell, L. M. Hartten, and A. C. Delany, 1998: The Flatland boundary layer experiments. *Bull. Amer. Meteor. Soc.,* **79,** 499–431, doi:10.1175/1520-0477(1998)079<0419:TFBLE>2.0.CO;2.

Ao, C. O., D. E. Waliser, S. K. Chan, J.-L. Li, B. Tian, F. Xie, and A. J. Mannucci, 2012: Planetary boundary layer heights from

GPS radio occultation refractivity and humidity profiles. *J. Geophys. Res.,* **117,** D16117, doi:10.1029/2012JD017598.

Beyrich, F., 1997: Mixing height estimation from sodar data—A critical discussion. *Atmos. Environ.,* **31,** 3941–3953, doi:10.1016/S1352-2310(97)00231-8.

Bianco, L., and J. M. Wilczak, 2002: Convective boundary layer depth: Improved measurement by Doppler radar wind profiler using fuzzy logic methods. *J. Atmos. Oceanic Technol.,* **19,** 1745–1758, doi:10.1175/1520-0426(2002)019<1745:CBLDIM>2.0.CO;2.

——, ——, and A. B. White, 2008: Convective boundary layer depth estimation from wind profilers: Statistical comparison between an automated algorithm and expert estimations. *J. Atmos. Oceanic Technol.,* **25,** 1397–1413, doi:10.1175/2008JTECHA981.1.

Bosilovich, M. G., 2013: Regional climate and variability of NASA MERRA and recent reanalyses: U.S. summertime precipitation and temperature. *J. Appl. Meteor. Climatol.,* **52,** 1939–1951, doi:10.1175/JAMC-D-12-0291.1.

Cohn, A. S., and W. M. Angevine, 2000: Boundary layer height and entrainment zone thickness measured by lidars and wind-profiling radars. *J. Appl. Meteor.,* **39,** 1233–1247, doi:10.1175/1520-0450(2000)039<1233:BLHAEZ>2.0.CO;2.

Compton, J. C., R. Delgado, T. A. Berkoff, and R. M. Hoff, 2013: Determination of planetary boundary layer height on short spatial and temporal scales: A demonstration of the covariance wavelet transform in ground-based wind profiler and lidar measurements. *J. Atmos. Oceanic Technol.,* **30,** 1566–1575, doi:10.1175/JTECH-D-12-00116.1.

Denning, A. S., T. Takahashi, and P. Friedlingstein, 1999: Can a strong atmospheric CO_2 rectifier effect be reconciled with a ''reasonable'' carbon budget? *Tellus,* **51B,** 249–253, doi:10.1034/j.1600-0889.1999.t01-1-00010.x.

Guo, P., Y.-H. Kuo, S. V. Sokolovskiy, and D. H. Lenschow, 2011: Estimating atmospheric boundary layer depth using COSMIC radio occultation data. *J. Atmos. Sci.,* **68,** 1703–1713, doi:10.1175/2011JAS3612.1.

Heo, B.-H., S. Jacoby-Koaly, K.-E. Kim, B. Campistron, B. Benech, and E.-S. Jung, 2003: Use of the Doppler spectral width to improve the estimation of the convective boundary layer height from UHF wind profiler observations. *J. Atmos. Oceanic Technol.,* **20,** 408–424, doi:10.1175/1520-0426(2003)020<0408:UOTDSW>2.0.CO;2.

Jordan, N. S., R. M. Hoff, and J. T. Bacmeister, 2010: Validation of Goddard Earth Observing System-version 5 MERRA planetary boundary layer heights using CALIPSO. *J. Geophys. Res.,* **115,** D24218, doi:10.1029/2009JD013777.

Lammert, A., and J. Bösenberg, 2006: Determination of the convective boundary-layer height with laser remote sensing. *Bound.-Layer Meteor.,* **119,** 159–170, doi:10.1007/s10546-005-9020-x.

Lewis, J. R., E. J. Welton, A. Molod, and E. Joseph, 2013: Improved boundary layer depth retrievals from MPLNET. *J. Geophys. Res. Atmos.,* **118,** 9870–9879, doi:10.1002/jgrd.50570.

Liu, S., and X.-Z. Liang, 2010: Observed diurnal cycle climatology of planetary boundary layer height. *J. Climate,* **23,** 5790–5809, doi:10.1175/2010JCLI3552.1.

OFCM, 1998: U.S. wind profilers: A review. Office of the Federal Coordinator for Meteorological Services and Supporting Research Tech. Rep. FCM-R14-1998, 57 pp.

McGrath-Spangler, E. L., and A. S. Denning, 2012: Estimates of North American summertime planetary boundary layer depths derived from space-borne lidar. *J. Geophys. Res.,* **117,** D15101, doi:10.1029/2012JD017615.

Rienecker, M. M., and Coauthors, 2011: MERRA: NASA's Modern-Era Retrospective Analysis for Research and Applications. *J. Climate,* **24,** 3624–3648, doi:10.1175/JCLI-D-11-00015.1.

Rossow, W. B., A. W. Walker, D. E. Beuschel, and M. D. Roiter, 1996: International Satellite Cloud Climatology Project (ISCCP): Documentation of new cloud datasets. WMO/TD-737, 115 pp. [Available online at http://isccp.giss.nasa.gov/pub/documents/d-doc.pdf.]

Seibert, P., F. Beyrich, S.-E. Gryning, S. Joffre, A. Rasmussen, and P. Tercier, 2000: Review and intercomparison of operational methods for the determination of the mixing height. *Atmos. Environ.,* **34,** 1001–1027, doi:10.1016/S1352-2310(99)00349-0.

Seidel, D. J., C. O. Ao, and K. Li, 2010: Estimating climatological planetary boundary layer heights from radiosonde observations: Comparison of methods and uncertainty analysis. *J. Geophys. Res.,* **115,** D16113, doi:10.1029/2009JD013680.

Simpson, M., S. Raman, J. K. Lundquist, and M. Leach, 2007: A study of the variation of urban mixed layer heights. *Atmos. Environ.,* **41,** 6923–6930, doi:10.1016/j.atmosenv.2006.08.029.

Singal, S. P., and M. Goel, 1997: Radio acoustic sounding system (RASS) for studying the lower atmosphere. *Acoustic Remote Sensing Applications,* S. P. Singal, Ed., Lecture Notes in Earth Sciences, Vol. 69, Narosa Publishing House, 142–176.

Spangler, T. C., and R. A. Dirks, 1974: Meso-scale variations of the urban mixing height. *Bound.-Layer Meteor.,* **6,** 423–441, doi:10.1007/BF02137677.

WMO, 2008: Measurement of humidity. WMO guide to meteorological instruments and methods of observation, WMO-8, Part I, I.4-1–I.4-30. [Available online at www.wmo.int/pages/prog/www/IMOP/CIMO-Guide.html.]